Assessing the Solution Shape and Size of Charged Dendronized Polymers Using Double Electron Electron Resonance.

Dennis Kurzbach[#], Daniel R. Kattnig[#], Baozhong Zhang[†], A. Dieter Schlüter[†], Dariush Hinderberger[#*]

[#]Max Planck Institute for Polymer Research, Ackermannweg 10, 55128 Mainz, Germany

[†]Department of Materials, Institute of Polymers, ETH Zurich, Wolfang-Pauli-Str. 10, HCI G525, Zurich 8093, Switzerland

*Corresponding Author: DH. E-Mail: dariush.hinderberger@mpip-mainz.mpg.de

- Supporting Information -

A. Additional Spectra and Figures

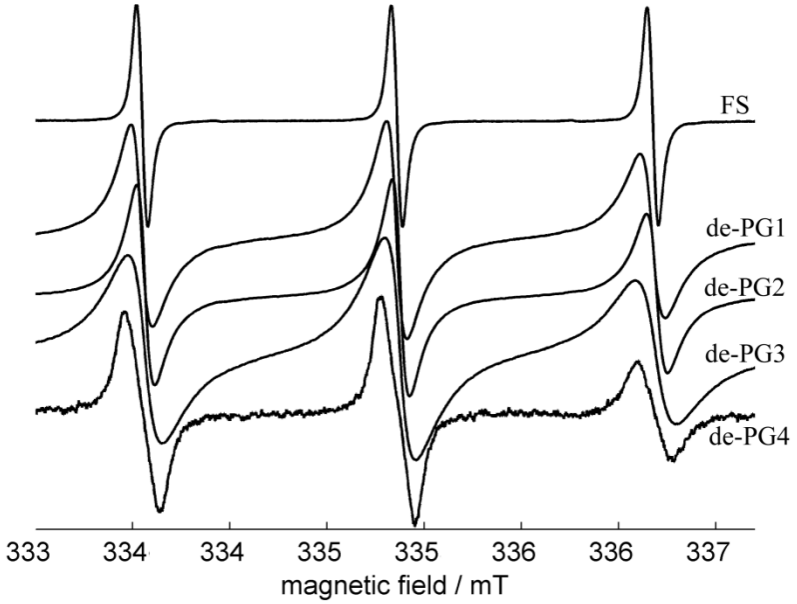

Figure S1: Continuous wave EPR spectra of 1 mM aqueous solutions of Fremy's Salt together with 1 wt % of the particular denpol generation. The rotational correlation time decreases with increasing generation.

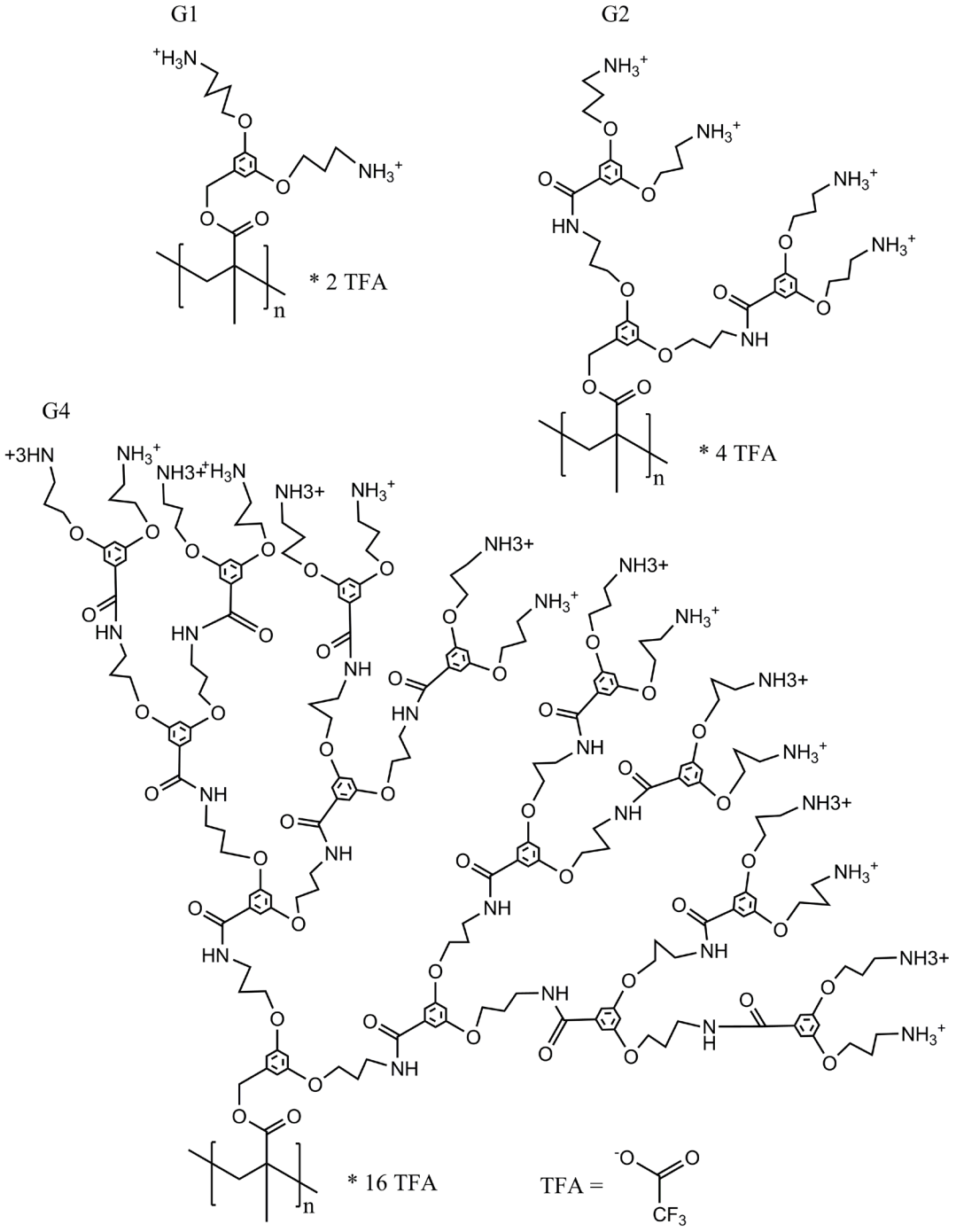

Figure S2: Molecular structures of the generations 1, 2 and 4 of the dendronized polymers used in this study.

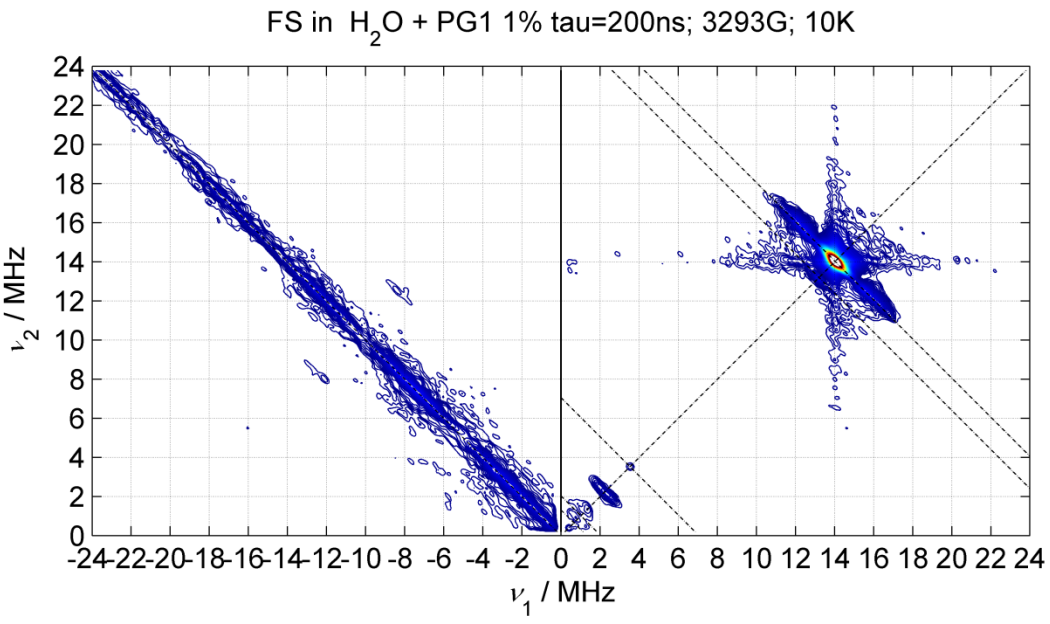

Figure S3: HYSCORE spectrum of FS on the generation 1 denpol at 10K. The ridge at 2 MHz indicates a weak coupling to a ^{14}N nucleus to the spin probes..

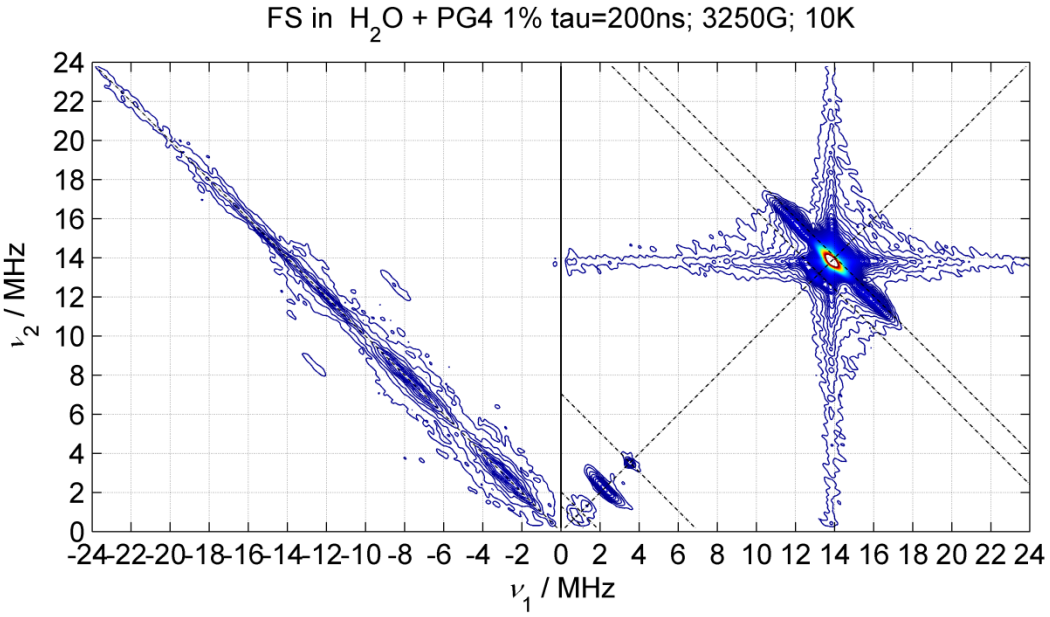

Figure S4: HYSCORE spectrum of FS on the generation 4 denpol at 10K. The ridge at 2 MHz indicates a weak coupling to a ^{14}N nucleus to the spin probes.

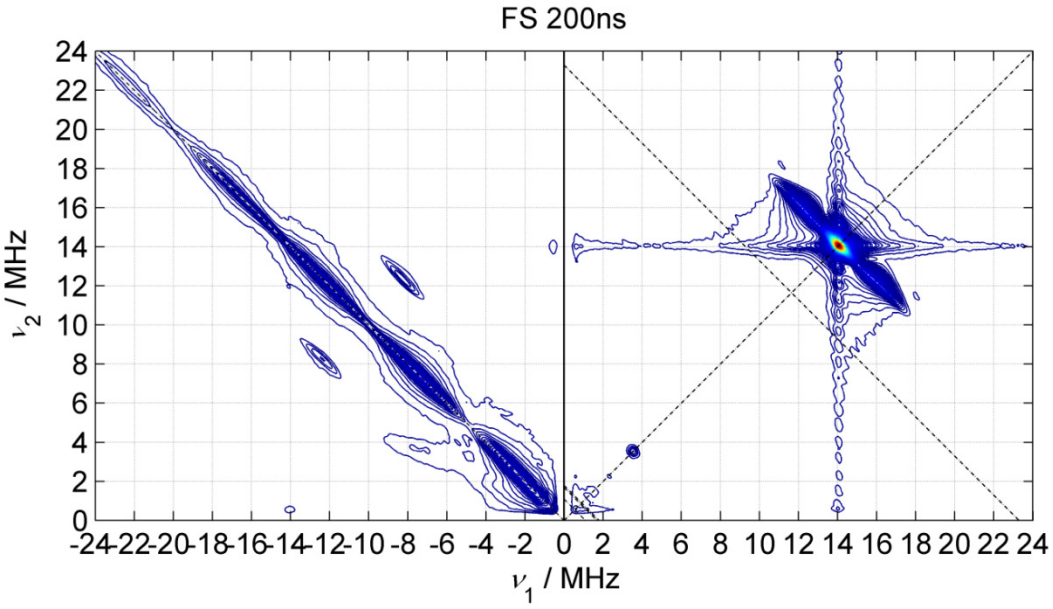

Figure S5: HYSCORE spectrum of FS at 10K. No additional ^{14}N couplings are visible.

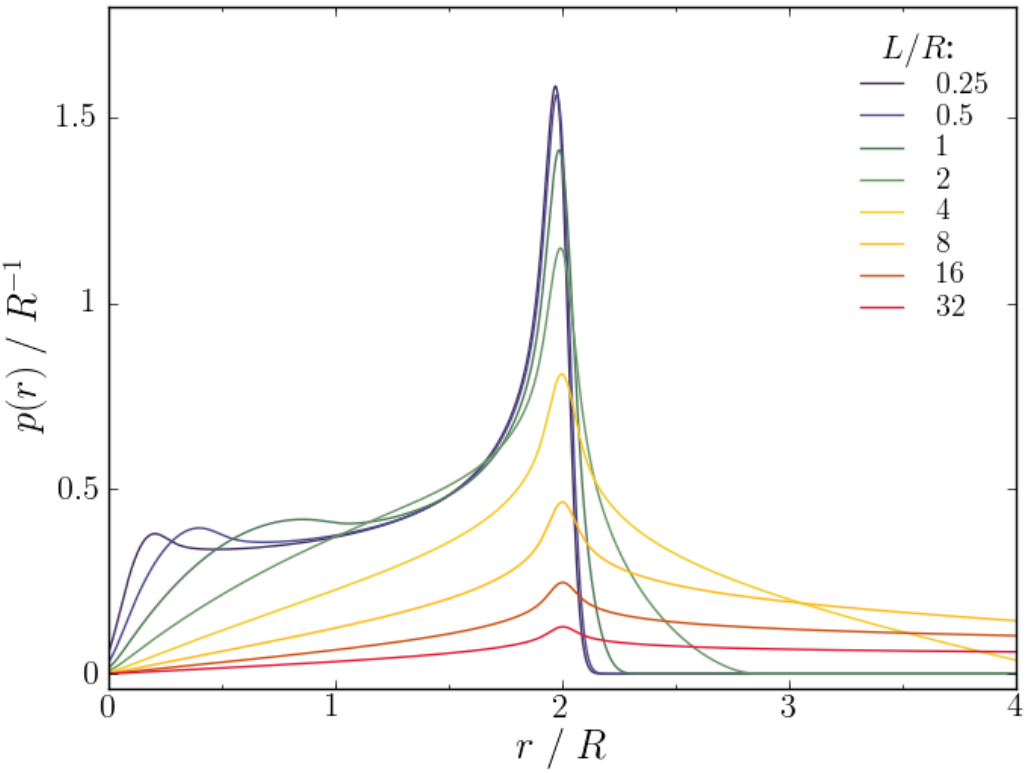

Figure S6: Distance distributions for different ratios of cylinder length L to radius R.

B. Sample Preparation and EPR Measurements.

All samples were prepared equally: We added small concentrations (2 mM) of Fremy's Salt, a two times negative charged spin-probe, to 1 wt % aqueous (or 0.5 % of both de-PG2 and de-PG4 for the mixture) solutions of four different generations of the denpols presented in Figure 1 and S2. HYSCORE and DEER is applied to glassy solids obtained by freeze-quenching the denpol solutions in supercooled isopentane. In this way a snapshot representative for the solution at room temperature is detected. The sample volume was always large enough to fill the complete resonator. A Miniscope MS200 (Magnettech, Berlin, Germany) benchtop spectrometer was used for X-band CW EPR measurements at a microwave frequency of ~9.4 GHz. Measurements were performed at room temperature (293 K) using a modulation amplitude of 0.05 mT. The microwave frequency was recorded with a frequency counter, model 2101 (Racal-Dana). The four pulse DEER sequence $\pi/2(\nu_{obs})$ - τ_1 - $\pi(\nu_{obs})$ - (τ_1 + t) - (ν_{pump}) - (τ_2 - t) - $\pi(\nu_{obs})$ - τ_2 - echo was used to obtain dipolar time evolution data at X-band frequencies (9.2 to 9.4 GHz) with a Bruker Elexsys 580 spectrometer equipped with a Bruker Flexline split-ring resonator ER4118X_MS3. The dipolar evolution time t was varied, whereas τ_2 = 2.5 μs and τ_1 were kept constant. Proton modulation was averaged by the addition of eight time traces of variable τ_1 , starting with $\tau_{1,0}$ = 200 ns and incrementing by $\Delta\tau_1$ = 8 ns. The resonator was overcoupled to Q = 100. The pump frequency, ν_{pump}, was set to the maximum of the EPR spectrum. The observer frequency, ν_{obs}, was set to ν_{pump}+ 61.6 MHz, coinciding with the lowfield local maximum of the nitroxide spectrum. The observer pulse lengths were 32 ns for both π/2 and π pulses, and the pump pulse length was 12 ns. The temperature was set to 50 K by cooling with a closed cycle cryostat (ARS AF204, customized for pulse EPR, ARS,Macungie, PA). The total measurement time for each sample was around 12 h. The raw time domain DEER data were processed with the program package DeerAnalysis2008. Intermolecular contributions were removed by division by an exponential decay with a dimension of d = 3. The resulting time traces were normalized to t = 0.

The parameter λ was determined by measuring DEER on a bi-radical, where Δ = λ and n = 2. λ was found to be 0.516.

HYSCORE experiments employed the pulse sequence $\pi/2-\tau-\pi/2-\tau_1-\pi-\tau_2-\pi/2-\tau echo$. The following parameters were used: mw pulses of lengths $t_{\pi/2} = t_{\pi}$= 16 ns, starting times 96 ns for t_1 and t_2, and time increments Δt = 16 ns (data matrix 256 × 256). Spectra with different τ values were recorded. An eight-step phase cycle was used to remove unwanted echoes. The HYSCORE data were processed with MATLAB 6.5 (The MathWorks, Inc.). The time traces were baseline corrected with an exponential, apodized with a Gaussian window and zero filled. After a two-dimensional Fourier transformation absolute-value spectra were calculated. Spectra recorded with different τ values were added to eliminate τ-dependent blind spots.
In all cases the temperature was set to 8 K by cooling with an ARS cryostat and closed-cycle cooling system. The samples were prepared as concentrated solutions (concentrations typically >10 mM) and the sample volume was always large enough to fill the complete resonator volume in the probehead (>300 μL).

C. The Distance Distributions of Particles on Cylinders

Given the highly-constrained molecular shapes of the dendronized polymers, we shall assume that the spin probes are distributed independently and uniformly on the lateral surface of right, circular cylinders. Working in dimensionless units with radius $R = 1$ and denoting the cylinder height by L the distance distribution is given by

$$P(r) = \frac{1}{L^2\pi}\int_0^L dz_1 \int_0^L dz_2 \int_0^\pi d\vartheta\, \delta(r - \sqrt{s(\vartheta)^2 + (z_1 - z_2)^2}) \tag{3}$$

Where $s(\vartheta) = 2\left|\sin\left(\vartheta/2\right)\right|$ is the cord length formed by two points on the circumference of the capping disk (of radius $R = 1$) subtending the angle ϑ. δ denotes the Dirac function. Eq. (3) is also equal to

$$P(r) = \frac{1}{L^2\pi}\int_0^L dz \int_0^2 ds\; \delta\left(r - \sqrt{s^2 + z^2}\right) P_c(s) P_l(z), \tag{4}$$

with

$$P_l(z) = \frac{2(L - z)}{L^2} \text{ and } P_c(s) = \frac{1}{\pi\sqrt{1 - \left(s/2\right)^2}} \tag{5}$$

denoting the probability densities that two points chosen by random on a line (length L) or the circumference of the unit-circle are separated by z or s, respectively. These probability density functions are easily evaluated from an ansatz analogous to eq. (3).[1, 2] Inserting eqs. (5) into eq. (4) and transforming the surface integral into a line integral over contours of constant $r = \sqrt{s^2 + z^2}$, we obtain

$$P(r) = \frac{2}{L^2\pi}\int_{r=\sqrt{s^2+z^2}} dl \frac{L - z}{\sqrt{1 - \left(s/2\right)^2}}, \tag{6}$$

where $dl = \sqrt{ds^2 + dz^2}$ is the line element. By parameterizing the contours via $z = r\cos\varphi$ and $s = r\sin\varphi$, the distance distribution results (for $r \le \sqrt{L^2 + 4}$):

$$\begin{aligned} P(r) &= \frac{2r}{L^2\pi}\int_{\Re\cos^{-1}(L/r)}^{\Re\sin^{-1}(2/r)} d\varphi \frac{L - r\cos(\varphi)}{\sqrt{1 - r^2\sin^2(\varphi)/4}} \\ &= \frac{2r}{L^2\pi}\left(L\,F\left(\varphi\middle| r^2/4\right) - 2\sin^{-1}\left(\frac{r}{2}\sin(\varphi)\right)\right)\Bigg|_{\Re\cos^{-1}(L/r)}^{\Re\sin^{-1}(2/r)}. \end{aligned} \tag{7}$$

Here, $F(\varphi|m)$ is the incomplete elliptic integral of the first kind and $\Re$ denotes the real part. Note that the modulus m also assumes values larger than 1 here. Eq. (7) assumes its maximum at $r = 2$ (where it is singular). Transforming eq. (7) to dimensional units, eq. (2) in the main manuscript is obtained. At the expense of conciseness, eq. (7) can easily expressed as piecewise function with 5 distinct domains. In practice we eventually convolute $P(r)$ as given by eq. (7) with a Gaussian broadening kernel. This is permitted for small broadenings since the exact asymptotic behavior for $r \to 0$ is elusive to DEER. This additional broadening is interpreted as to account for the fluxionally/mobility of the probe, dispersion of

the cylinder radius, etc.[3] Figure S6 depicts an illustration of the shapes of the distance distributions so obtained and their dependence on *L*.

D. Corrections of Cylinder Radii Based on the Poisson-Boltzmann Equation

The interplay of thermal motion and attractive electrostatic interactions leads to a *statistical distribution* of the charged spin probe about the polyelectrolyte/denpol. Besides the *finite size* of the probe, this non-covalent attachment gives rise to larger distances in the DEER distance distribution than would be expected on the basis of the molecular object under study. Given the well-defined molecular shape of the denpols de-PG1 to de-PG4, this overestimate of *R* can be compensated easily: Within the mean-field picture, the distribution of the probe about the denpol strands, and hence a judicious correction to *R*, can be determined on the basis of the non-linear Poisson-Boltzmann equation.[4] We shall employ the cylindrical cell model (Manning-Onsager model). To this end the polyelectrolyte solution is modeled as being assembled from cylindrical cells containing the cylindrical polyions along their axes and all counterioins (here: trifluoroacetate) and co-ions (potassium and the FS anion) within the surrounding dielectric. In detail, the Poisson-Boltzmann equation for the electrostatic potential, $\varphi(r)$, is solved in the form

$$\frac{1}{r}\frac{d}{dr}r\frac{d\varphi(r)}{dr} = -\frac{e}{\varepsilon_0\varepsilon_r}\sum_i z_i n_i(b)\exp\left(-\beta e z_i\varphi(r)\right). \tag{8}$$

Here, $\beta = (k_B T)^{-1}$, and the sum runs over all mobile electrolytes of charge number z_i (co-ions and counterions, 3 summands). $n_i(b)$ is the number density of the ionic species *i* at the location for which $\varphi = 0$. We (arbitrarily) enforce $\varphi(b) = 0$ at the outer cell boundary, *b*. The n_i(b)s deviate significantly from the macroscopic concentration due to the condensation of the counterions at the denpoly boundary. Self-consistency is ensured by requiring that the number of ionic species within the cell (macroscopic concentration c_i, volume V_z), $c_i V_z N_A$, fulfills

$$c_i V_z N_A = 2\pi n_i(b)\int_a^b r\exp\left(-\beta e z_i\varphi(r)\right)dr. \tag{9}$$

The inner domain radius, *a*, equals the average contact distance of the polycation and the co-ions, i.e. $a = R + r_{ion}$, with *R* denoting the (true) denpol radius. r_{ion} = 1.5 Å (half the S-S distance in FS) has been assumed here. The outer boundary radius, *b*, is evaluated from the concentration of repeat units, i.e. $c_{RU} = 1/(\pi b^2 N_A h)$, where *h* is the height of the repeat unit. The boundary conditions follow from Gauss' law:

$$\left.\frac{d\varphi}{dr}\right|_{r=a} = -\frac{\sigma}{\varepsilon_0\varepsilon_r} \quad \text{and} \quad \left.\frac{d\varphi}{dr}\right|_{r=b} = 0, \tag{10}$$

with σ denoting surface charge density of the polycation. The second condition reflects the electro-neutrality of the cylindrical cell. No analytical solution of eqs. (8) and (10) is available. With the numerical solution in mind, it is convenient to transform the equation by introducing the dimensionless quantities $y = e\beta\varphi$ and $x = \ln(r/a)$. The transformed differential equation reads:

$$\frac{d^2y(x)}{dx^2} = -4\pi L_B a^2\sum_i z_i n_i(b)\exp\left(-z_i y(x) + 2x\right), \tag{11}$$

where the Bjerrum length is defined by $L_B = e^2\beta/(4\pi\varepsilon_0\varepsilon_r)$. L_B = 7.1 Å for water at 293K. The transformed boundary conditions are:

$$\left.\frac{dy}{dx}\right|_{x=0} = -2\xi = -2z_{RU}\frac{L_B}{h} \quad \text{and} \quad \left.\frac{dy}{dx}\right|_{x=\ln(b/a)} = 0\,. \tag{12}$$

The linear charge parameter, ξ, is related to the charge, $e\xi$, of a cylinder of height L_B.

The boundary value problem is solved using a home-written Matlab program. The bvp4c routine (Lobatto collocation) is used to solve eqs. (11) and (12) for given values of the number density at b, $n_i(b)$. A shift parameter of the potential is introduced, that enforces $\varphi(b) = 0$ (in addition to the boundary conditions given by eq. (12)). Self-consistency is established in an iterative process. In every iteration the $n_i(b)$s are updated using eq. (9). This process is continued until no significant change in the potential is observed. The average cylinder radius, is then determined from

$$\left\langle R_{DEER} \right\rangle = \frac{\int_a^{r_{\max}} r^2 \exp\left(-z_i\beta\varphi(r)\right) dr}{\int_a^{r_{\max}} r \exp\left(-z_i\beta\varphi(r)\right) dr}, \tag{13}$$

where r_{max} = 8 nm, i.e. the upper bound of distances currently attainable by DEER. Note that the potential is quasi entirely shielded at large distances and hence the number of particles at large radii increases just because of the increase in phase-space volume. However, these particles at large distances do only contribute to the DEER background. Following this approach, corrections to the cylinder radius have been evaluated for the pertinent experimental conditions. The projected radius, the surface charge density and, hence, the repeat unit height, the concentrations of electrolytes, and the co-ion radius determine the size of the correction. Table 1 summarizes the correction factors using the R_{AFM}s and the repeat unit heights for the protected PG denpols as starting point[5,6] Using R_{DEER} instead of R_{AFM} gives concordant results. Note that primarily due to the increase in h with generation, the correction amounts to approximately 3 Å for *all* systems.

Table 1: Correction factors, Δ, for the cylinder radius resulting from the Poisson-Boltzmann treatment of the charge distribution of FS about cylindrical polycations and the parameters used for their derivation. In addition, c_{FS} = 2 mM, L_B = 7.1 Å.

generation	a / Å	z_{RU}	c_{RU} / mM	D / Å
1	3.5	2	1.9	-3.4
2	6.5	4	0.84	-2.9
3	12.5	8	0.39	-3.0
4	21.5	16	0.19	-3.4

References.

1. Arfken, G., Mathematical Methods for Physicists, Academic Press, Orlando, FL, 1985.
2. Weisstein, E. W., CRC Concise Encyclopedia of Mathematics, Second Edition, Chapman & Hall/CRC, Boca Raton, FL, 2002; http://mathworld.wolfram.com/.
3. This approach is approximate in the sense that it gives rise to negative distances. Since distances smaller than approximately 1 nm are elusive to the DEER method, no significant error is introduced in the results. On the other hand, the faster computation time outweighs the merits of the more exact approach of co-adding cylinder distance distributions of different r weighted by a Gaussian distribution.
4. Alexandrowicz Z. and Katchalsky A. *J. Polymer Sci. A*, **1963**, *1*, 3231-3260.
5. Zhang, B.; Wepf, R.; Fischer, K.; Schmidt, M.; Besse, S.; Lindner, P.; King, B. T.; Sigel, R.; Schurtenberger, P.; Talmon, Y.; Ding, Y.; Kröger, M.; Halperin, A.; Schlüter, A. D. *Angew. Chem. Int. Ed*. **2011**, *50*, 737.
6. Zhang, A.; Okrasa L.; Pakula T.; Schlüter A. D. *J. Amer. Chem. Soc*. **2004**, *126*, 6658.